Available at www.MATHEMATICSweb.org
POWERED BY SCIENCE @ DIRECT®

Journal of Computational and Applied Mathematics 155 (2003) 263–284

JOURNAL OF COMPUTATIONAL AND APPLIED MATHEMATICS

www.elsevier.com/locate/cam

Constructing smoothing functions in smoothed particle hydrodynamics with applications

M.B. Liu[a,*], G.R. Liu[a], K.Y. Lam[b]

[a] *Center for ACES, Department of Mechanical Engineering, National University of Singapore, 10 Kent Ridge Crescent, Singapore 119260, Singapore*

[b] *Institute of High Performance Computing, 1 Science Park Road, #01-01 The Capricorn, Singapore Science Park II, Singapore 117528, Singapore*

Received 1 February 2002; received in revised form 19 October 2002

Abstract

This paper presents a general approach to construct analytical smoothing functions for the meshfree, Lagrangian and particle method of smoothed particle hydrodynamics. The approach uses integral form of function representation and applies Taylor series expansion to the SPH function and derivative approximations. The constructing conditions are derived systematically, which not only interpret the consistency condition of the method, but also describe the compact supportness requirement of the smoothing function. Examples of SPH smoothing function are constructed including some existing ones. With this approach, a new quartic smoothing function with some advantages is constructed, and is applied to the one dimensional shock problem and a one dimensional TNT detonation problem. The good agreement between the SPH results and those from other sources shows the effectiveness of the approach and the newly constructed smoothing function in numerical simulations.

Keywords: Smoothed particle hydrodynamics; Smoothing function; Constructing condition; Hydrodynamic simulation

1. Introduction

The smoothed particle hydrodynamics (SPH) method, as a truly meshfree, free Lagrangian, particle method, offers substantial potential in many classes of problems especially those characterized by large deformations and moving discontinuities. Since its invention to solve astrophysical problems in three dimensional open space [11,3], SPH has been extensively studied and extended to dynamic

* Corresponding author. Tel.: +65-6874-4796; fax: +65-6874-4795.
E-mail address: mpeliumb@nus.edu.sg (M.B. Liu).

0377-0427/03/$ - see front matter
doi:10.1016/S0377-0427(02)00869-5

response with material strength [7,6], free surface flows [13,23], explosion phenomena [10], heat transfer and mass flow [2] and many other applications. Different parallel computing techniques have been employed to enhance the performance of the SPH method [4,18,1].

One of the central issues for the meshfree methods is how to effectively construct a proper shape function using only nodes scattered in an arbitrary manner without using a predefined mesh that provides the connectivity of the nodes. For smoothed particle hydrodynamics (SPH) method, the smoothing function (also called smoothing kernel, smoothing kernel function or simply kernel in many SPH literatures) is of utmost importance since it not only determines the pattern to interpolate, but also defines the width of the influencing area of a particle. Different smoothing functions have been used in the SPH method as shown in published literatures and informal papers. Various requirements or properties for the smoothing function are applied in different literatures. Summarized below are the most general ones:

1. The smoothing function must be normalized,
$$\int W(\boldsymbol{x}-\boldsymbol{x}',h)\,\mathrm{d}\boldsymbol{x}'=1, \tag{1}$$
where $W(\boldsymbol{x}-\boldsymbol{x}',h)$ is the smoothing function, $\boldsymbol{x}$ is the position vector. h is the smoothing length that determines the supporting area of the smoothing function.
2. The smoothing function should have compact supportness. In general, the compact supportness is defined by the smoothing length h and a scale factor κ that determines the spread of the specified smoothing function. So the compact supportness means
$$W(\boldsymbol{x}-\boldsymbol{x}')=0 \quad \text{for } |\boldsymbol{x}-\boldsymbol{x}'|>\kappa h, \tag{2}$$
3. $W(\boldsymbol{x}-\boldsymbol{x}')\geqslant 0$ in the compact supportness area of $|\boldsymbol{x}-\boldsymbol{x}'|\leqslant \kappa h$.
4. The smoothing function should be monotonically decreasing.
5. The smoothing function should satisfy the Dirac delta function condition as $h\to 0$.
$$\lim_{h\to 0} W(\boldsymbol{x}-\boldsymbol{x}',h)=\delta(\boldsymbol{x}-\boldsymbol{x}'). \tag{3}$$
6. The smoothing function should be an even (symmetric) function.
7. The smoothing function should be sufficiently smooth.
8. The smoothing function should be of the form $W(\boldsymbol{x}-\boldsymbol{x}',h)=\alpha_{\mathrm{d}}K(S)$, where α_{d} is the dimension-dependent normalization constant for particular smoothing kernel functions, $S=|\boldsymbol{x}-\boldsymbol{x}'|/h$.

Any function having the above properties can be employed as an SPH smoothing kernel function. Although Monaghan [12] stated that to find a physical interpretation of an SPH equation, it is always best to assume the smoothing function to be a Gaussian, many researchers and practitioners ever tried different kinds of smoothing functions. This paper gives a general approach to construct smoothing function. The constructing conditions are systematically derived, which, on the one hand, interpret the consistency conditions of the SPH method, on the other hand, determine the compact supportness of the smoothing function. The effectiveness of this approach is demonstrated by a series of constructed smoothing functions, which include some existent ones and a new quartic smoothing function. The new quartic smoothing function is applied to simulate the one dimensional shock tube problem and a one dimensional TNT detonation problem with fairly good results.

2. Constructing conditions

Any numerical approximation should represent the corresponding physical equations. In the traditional finite difference methods (FDM), the concept of consistency defines how well the numerical equations model the physical equations. A numerical interpolation scheme (in FDM) is consistent if it has the ability to exactly represent the differential equations in the limit as the number of the grid point approaches infinity and the maximal mesh size approaches zero. On the one hand, consistency is the basic requirement to construct a finite difference scheme, on the other hand, consistency is a prerequisite for convergence, since according to the Lax–Richtmyer equivalence theorem, and a consistent finite difference scheme for a well-posed partial differential equation is convergent if and only if it is stable. Similarly, by using the Taylor series expansion, analysis can be carried out on how well the SPH approximation models the physical equations in the limit as the number of the particles approaches infinite and the smoothing length approaches zero. This analysis is carried out in the stage of SPH kernel approximation for a function and its derivatives. The analysis shows that to exactly approximate a function and its derivatives, certain conditions need to be satisfied, which can be used to construct smoothing functions.

2.1. Approximating the function

In the SPH method, for a function f, multiplying f with the smoothing kernel function W, and then integrating over the computational domain can approximate its function value at a certain point.

$$f(\boldsymbol{x}) = \int f(\boldsymbol{x}')W(\boldsymbol{x}-\boldsymbol{x}',h)\,\mathrm{d}\boldsymbol{x}'. \tag{4}$$

Suppose $f(\boldsymbol{x})$ is sufficiently smooth, applying Taylor series expansion to $f(\boldsymbol{x}')$ in the integration in Eq. (4) around $\boldsymbol{x}$ yields

$$\begin{aligned} f(\boldsymbol{x}') &= f(\boldsymbol{x}) + f'(\boldsymbol{x})(\boldsymbol{x}'-\boldsymbol{x}) + \frac{1}{2}f''(\boldsymbol{x})(\boldsymbol{x}'-\boldsymbol{x})^2 + \cdots \\ &= \sum_{k=0}^{n} \frac{(-1)^k h^k f^{(k)}(\boldsymbol{x})}{k!}\left(\frac{\boldsymbol{x}-\boldsymbol{x}'}{h}\right)^k + r_n\left(\frac{\boldsymbol{x}-\boldsymbol{x}'}{h}\right), \end{aligned} \tag{5}$$

where $r_n((\boldsymbol{x}-\boldsymbol{x}')/h)$ is the remainder of the Taylor series expansion. Substituting Eq. (5) into Eq. (4) yields

$$f(\boldsymbol{x}) = \sum_{k=0}^{n} A_k f^{(k)}(\boldsymbol{x}) + r_n\left(\frac{\boldsymbol{x}-\boldsymbol{x}'}{h}\right), \tag{6}$$

$$A_k = \frac{(-1)^k h^k}{k!}\int \left(\frac{\boldsymbol{x}-\boldsymbol{x}'}{h}\right)^k W(\boldsymbol{x}-\boldsymbol{x}',h)\,\mathrm{d}\boldsymbol{x}'. \tag{7}$$

Comparing the LHS with the RHS of Eq. (6), in order for $f(\boldsymbol{x})$ to be approximated to nth order, the coefficients A_k must be equal to the counterparts for $f^{(k)}(\boldsymbol{x})$ in the LHS of Eq. (6), and therefore result in the following conditions:

$$A_0 = \int W(\boldsymbol{x} - \boldsymbol{x}', h)\,\mathrm{d}\boldsymbol{x}' = 1,$$

$$A_1 = h \int \left(\frac{\boldsymbol{x} - \boldsymbol{x}'}{h}\right) W(\boldsymbol{x} - \boldsymbol{x}', h)\,\mathrm{d}\boldsymbol{x}' = 0$$

$$\vdots$$

$$A_n = \frac{(-1)^n h^n}{n!} \int \left(\frac{\boldsymbol{x} - \boldsymbol{x}'}{h}\right)^n W(\boldsymbol{x} - \boldsymbol{x}', h)\,\mathrm{d}\boldsymbol{x}' = 0 \tag{8}$$

or the following simplified expressions in terms of the moments M_k:

$$M_0 = \int W(\boldsymbol{x} - \boldsymbol{x}', h)\,\mathrm{d}\boldsymbol{x}' = 1,$$

$$M_1 = \int (\boldsymbol{x} - \boldsymbol{x}') W(\boldsymbol{x} - \boldsymbol{x}', h)\,\mathrm{d}\boldsymbol{x}' = 0$$

$$\vdots$$

$$M_n = \int (\boldsymbol{x} - \boldsymbol{x}')^n W(\boldsymbol{x} - \boldsymbol{x}', h)\,\mathrm{d}\boldsymbol{x}' = 0. \tag{9}$$

2.2. Approximating the derivatives

In the computational fluid dynamics (CFD), since the highest derivative is second order, in the following discussions, only the first and second order derivatives are concerned. This is because, on the one hand, the procedure can be easily extended to approximate higher derivatives and obtain similar results, on the other hand, one can regard a higher derivative as the derivative of a lower derivative (e.g., second derivative is the derivative of the first derivative, and so on).

The approximation of the first derivative in SPH can be obtained by replacing the function $f(\boldsymbol{x})$ in (4) with the derivative $f'(\boldsymbol{x})$,

$$f'(\boldsymbol{x}) = \int f'(\boldsymbol{x}') W(\boldsymbol{x} - \boldsymbol{x}', h)\,\mathrm{d}\boldsymbol{x}'. \tag{10}$$

By using integration by parts, the above equation can be rewritten as

$$f'(\boldsymbol{x}) = \int_s f(\boldsymbol{x}') W(\boldsymbol{x} - \boldsymbol{x}', h) \cdot \vec{\boldsymbol{n}}\,\mathrm{d}s - \int f(\boldsymbol{x}') W'(\boldsymbol{x} - \boldsymbol{x}', h)\,\mathrm{d}\boldsymbol{x}', \tag{11}$$

where $\vec{\boldsymbol{n}}$ is the unit vector normal to the surface. The first integral is over the surface s of the computational domain. Substituting (5) into the second integral on the RHS of Eq. (11) yields

$$f'(\boldsymbol{x}) = \int_s f(\boldsymbol{x}') W(\boldsymbol{x} - \boldsymbol{x}', h) \cdot \vec{\boldsymbol{n}}\,\mathrm{d}s + \sum_{k=0}^{n} A'_k f^{(k)}(\boldsymbol{x}) + r_n \left(\frac{\boldsymbol{x} - \boldsymbol{x}'}{h}\right), \tag{12}$$

$$A'_k = \frac{(-1)^{k+1} h^k}{k!} \int \left(\frac{\boldsymbol{x} - \boldsymbol{x}'}{h}\right)^k W'(\boldsymbol{x} - \boldsymbol{x}', h)\,\mathrm{d}\boldsymbol{x}'. \tag{13}$$

Similarly, if the following equations are satisfied, $f'(\boldsymbol{x})$ can be approximated to nth order,

$$M'_0 = \int W'(\boldsymbol{x}-\boldsymbol{x}',h)\,\mathrm{d}\boldsymbol{x}' = 0,$$

$$M'_1 = \int (\boldsymbol{x}-\boldsymbol{x}')W'(\boldsymbol{x}-\boldsymbol{x}',h)\,\mathrm{d}\boldsymbol{x}' = 1$$

$$\vdots$$

$$M'_n = \int (\boldsymbol{x}-\boldsymbol{x}')^n W'(\boldsymbol{x}-\boldsymbol{x}',h)\,\mathrm{d}\boldsymbol{x}' = 0, \tag{14}$$

$$W_s(\boldsymbol{x}-\boldsymbol{x}',h) = 0. \tag{15}$$

Eq. (15) defines the smoothing function value on the surface to be zero, which determines the surface integration $\int_s f(\boldsymbol{x}')W(\boldsymbol{x}-\boldsymbol{x}',h)\cdot\vec{\boldsymbol{n}}\,\mathrm{d}s$ to vanish for arbitrarily selected function $f(\boldsymbol{x})$. The first expression in Eq. (14) is actually another representation of Eq. (15) as we can see from the following expression:

$$\int W'(\boldsymbol{x}-\boldsymbol{x}',h)\,\mathrm{d}\boldsymbol{x}' = \int 1\cdot W(\boldsymbol{x}-\boldsymbol{x}',h)\cdot\vec{\boldsymbol{n}}\,\mathrm{d}s - \int (1)'\cdot W(\boldsymbol{x}-\boldsymbol{x}',h)\,\mathrm{d}\boldsymbol{x}'$$
$$= \int_s^s W(\boldsymbol{x}-\boldsymbol{x}',h)\cdot\vec{\boldsymbol{n}}\,\mathrm{d}s = 0. \tag{16}$$

The approximation of the second derivative can be obtained similarly by directly substituting the function $f(\boldsymbol{x})$ in (4) with the derivative $f''(\boldsymbol{x})$. After using integration by parts, the following expressions can be derived in order to approximate $f''(\boldsymbol{x})$ to nth order:

$$M''_0 = \int W''(\boldsymbol{x}-\boldsymbol{x}',h)\,\mathrm{d}\boldsymbol{x}' = 0,$$

$$M''_1 = \int (\boldsymbol{x}-\boldsymbol{x}')W''(\boldsymbol{x}-\boldsymbol{x}',h)\,\mathrm{d}\boldsymbol{x}' = 0,$$

$$M''_2 = \int (\boldsymbol{x}-\boldsymbol{x}')^2 W''(\boldsymbol{x}-\boldsymbol{x}',h)\,\mathrm{d}\boldsymbol{x}' = 2$$

$$\vdots$$

$$M''_n = \int (\boldsymbol{x}-\boldsymbol{x}')^n W''(\boldsymbol{x}-\boldsymbol{x}',h)\,\mathrm{d}\boldsymbol{x}' = 0, \tag{17}$$

$$W_s(\boldsymbol{x}-\boldsymbol{x}',h) = 0, \tag{18}$$

$$W'_s(\boldsymbol{x}-\boldsymbol{x}',h) = 0. \tag{19}$$

Again, Eqs. (18) and (19) determine the surface term to vanish for arbitrarily selected function $f(\boldsymbol{x})$ and its first derivative $f'(\boldsymbol{x})$. The first expression in Eq. (17) is actually another representation of Eq. (19) as we can see from the following expression:

$$\int W''(\boldsymbol{x}-\boldsymbol{x}',h)\,\mathrm{d}\boldsymbol{x}' = \int_s 1\cdot W'(\boldsymbol{x}-\boldsymbol{x}',h)\cdot\vec{\boldsymbol{n}}\,\mathrm{d}s - \int (1)'\cdot W'(\boldsymbol{x}-\boldsymbol{x}',h)\,\mathrm{d}\boldsymbol{x}'$$
$$= \int_s^s W'(\boldsymbol{x}-\boldsymbol{x}',h)\cdot\vec{\boldsymbol{n}}\,\mathrm{d}s = 0. \qquad (20)$$

If Eqs. (18) and (19) are satisfied, Eq. (14) and (17) can be derived from Eq. (9) (except the first one expression in (14) and first two expressions in (17)) by using the integration by parts with some trivial transformations

$$\int (\boldsymbol{x}-\boldsymbol{x}')^k W(\boldsymbol{x}-\boldsymbol{x}',h)\,\mathrm{d}\boldsymbol{x}' = \frac{1}{(k+1)}\int (\boldsymbol{x}-\boldsymbol{x}')^{k+1} W'(\boldsymbol{x}-\boldsymbol{x}',h)\,\mathrm{d}\boldsymbol{x}'$$
$$= \frac{1}{(k+1)(k+2)}\int (\boldsymbol{x}-\boldsymbol{x}')^{k+2} W''(\boldsymbol{x}-\boldsymbol{x}',h)\,\mathrm{d}\boldsymbol{x}'. \qquad (21)$$

In sum, if a function and its first two derivatives are to be reproduced to nth order accuracy, then the smoothing function should satisfy

$$M_0 = \int W(\boldsymbol{x}-\boldsymbol{x}',h)\,\mathrm{d}\boldsymbol{x}' = 1,$$
$$M_1 = \int (\boldsymbol{x}-\boldsymbol{x}')W(\boldsymbol{x}-\boldsymbol{x}',h)\,\mathrm{d}\boldsymbol{x}' = 0$$
$$\vdots$$
$$M_n = \int (\boldsymbol{x}-\boldsymbol{x}')^n W(\boldsymbol{x}-\boldsymbol{x}',h)\,\mathrm{d}\boldsymbol{x}' = 0, \qquad (22)$$

$$W_s(\boldsymbol{x}-\boldsymbol{x}',h) = 0,$$
$$W_s'(\boldsymbol{x}-\boldsymbol{x}',h) = 0. \qquad (23)$$

It can be seen that the constructing conditions can be classified into two groups. The first group shows the ability of the smoothing function to reproduce polynomials and thus is the representation of the consistency concept that will be further discussed later. With the first group, the function can be exactly approximated to nth order. The second group defines the surface value of the smoothing function as well as its first derivative, and is the representation of the property of compact support for the smoothing function and its first derivative. With these constructing conditions, the function as well as its first two derivatives can be exactly approximated to nth order. The constructing conditions for higher order derivatives of a function can be obtained in the same procedure, and can also be classified into two similar groups. Except from the constructing conditions expressed in Eq. (22), (23), the higher order derivatives of smoothing function should have also compact support like Eq. (23).

Revisiting the previously listed properties of the smoothing function, the normalization property expressed in Eq. (1) is actually a constituent of Eq. (22). The compact supportness property of the smoothing function is also a constituent of the surface Eqs. (23). It is clear that the previously discussed requirements on the smoothing function are actually the representations of SPH approximation for a function and its derivatives.

2.3. Consistency

The constructing conditions shown in Eqs. (22) and (23) are derived by using Taylor series expansion. With such constructing conditions satisfied, the SPH approximations for a function and its derivative can be consistent to a given order. This Taylor series expansion based approach is somewhat similar to the consistency concept for the traditional finite difference method in treating partial differential equations (PDE) in strong form.

Similarly, the consistency concept for the traditional finite element methods (FEM) also applies to the meshfree particle methods. In general, in FEM, if an approximation can reproduce a polynomial of up to kth order exactly, the approximation is said to have kth order consistency or C^k consistency. Borrowing the consistency concept from FEM, we may say that for an SPH approximation to exactly reproduce a function, the smoothing function should have certain degree of consistency, which again can be represented by its ability to reproduce the polynomials. For a constant field $f(\boldsymbol{x}) = c$ to be reproduced, according to the SPH kernel approximation, we obtain

$$f(\boldsymbol{x}) = \int cW(\boldsymbol{x} - \boldsymbol{x}', h)\,\mathrm{d}\boldsymbol{x}' = c, \tag{24}$$

or

$$\int W(\boldsymbol{x} - \boldsymbol{x}', h)\,\mathrm{d}\boldsymbol{x}' = 1. \tag{25}$$

It is clear that the normalization condition or the first expression in (22) is actually the representation of the zeroth order consistency.

It is easy to show that other constructing conditions shown in Eq. (22) can also be regarded as the high order consistency condition. Let's consider a single term of the polynomial k ($k \geqslant 1$) or simply assume $f(\boldsymbol{x}) = c_k \boldsymbol{x}^k$, approximating the function value at the origin $x = 0$ yields

$$f(0) = \int c\boldsymbol{x}'^k W(0 - \boldsymbol{x}', h)\,\mathrm{d}\boldsymbol{x}' = 0. \tag{26}$$

The general expression can be obtained by moving the origin to a certain point to get the approximation of the function at the origin in the new coordinate system, so

$$\int (\boldsymbol{x} - \boldsymbol{x}')^k W(\boldsymbol{x} - \boldsymbol{x}', h)\,\mathrm{d}\boldsymbol{x}' = 0. \tag{27}$$

It is clear that Eq. (27) is the same as Eq. (22). Therefore the constructing conditions shown in Eq. (22) can also be regarded as the consistency conditions.

2.4. Further discussions

The above discussed consistency expressions are derived from the continuous form (integral with the kernel or kernel approximation). They do not assure consistency for the discrete form (particle

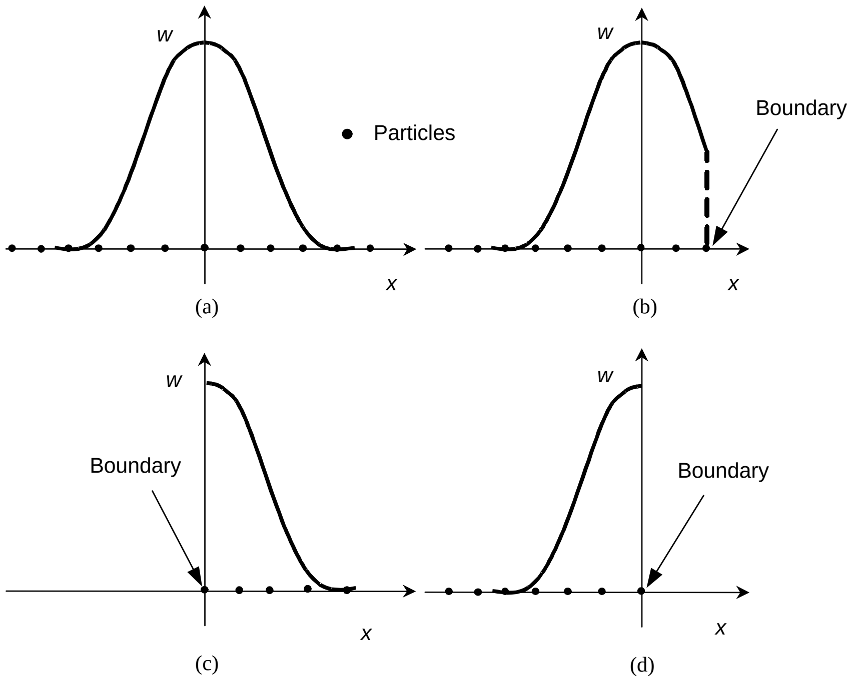

Fig. 1. Illustration of particle inconsistency of SPH for one dimensional case with regular particle distribution. (a) For an interior point; (b), (c) and (d) for a point near the boundary or on the boundaries.

approximation). In meshfree particle methods this phenomenon is called particle inconsistency. The discrete counterpart of the constant and linear consistency conditions are

$$\sum_{j}^{N} W(\boldsymbol{x}-\boldsymbol{x}_j,h)\Delta\boldsymbol{x}_j = 1, \tag{28}$$

$$\sum_{j}^{N} (\boldsymbol{x}-\boldsymbol{x}_j)W(\boldsymbol{x}-\boldsymbol{x}_j,h)\Delta\boldsymbol{x}_j = 0, \tag{29}$$

where N is the total number of neighbour particles for the given particle locating at $\boldsymbol{x}$. These discretized consistency conditions are not always satisfied. One direct and simple case is for the particles at or near the boundaries, as clearly shown on Fig. 1, even for regular node (particle) distribution, due to the inefficient particles contributing to the discretized summation, the LHS of Eq. (28) is less than 1 and the LHS of Eq. (29) will not vanish to be zero. It can also be easily shown that for irregular particle distribution, even for the interior particles, the constant and linear consistency condition in the discretized form will not be exactly satisfied. Similarly the discrete counterparts of higher order consistency conditions are also not always exactly satisfied.

There are different means to restore the consistency condition for the discrete form. One possible approach is given here. For a particle approximation to obtain kth order consistency in discrete form, we may take the smoothing function as

$$W(\boldsymbol{x}-\boldsymbol{x}_j,h)=b_0(\boldsymbol{x},h)+b_1(\boldsymbol{x},h)\left(\frac{\boldsymbol{x}-\boldsymbol{x}_j}{h}\right)+b_2(\boldsymbol{x},h)\left(\frac{\boldsymbol{x}-\boldsymbol{x}_j}{h}\right)^2+\cdots$$
$$=\sum_{I=0}^{k} b_I(\boldsymbol{x},h)\left(\frac{\boldsymbol{x}-\boldsymbol{x}_j}{h}\right)^I. \tag{30}$$

The discretized form for Eq. (22) can be rewritten as

$$\sum_{I=0}^{k} b_I(\boldsymbol{x},h)\sum_{j}^{N}\left(\frac{\boldsymbol{x}-\boldsymbol{x}_j}{h}\right)^I \Delta\boldsymbol{x}_j=1$$
$$\vdots$$
$$\sum_{I=0}^{k} b_I(\boldsymbol{x},h)\sum_{j}^{N}\left(\frac{\boldsymbol{x}-\boldsymbol{x}_j}{h}\right)^{I+k} \Delta\boldsymbol{x}_j=0. \tag{31}$$

Assuming

$$m_k(\boldsymbol{x},h)=\sum_{j}^{N}\left(\frac{\boldsymbol{x}-\boldsymbol{x}_j}{h}\right)^k \Delta\boldsymbol{x}_j,$$

the $k+1$ coefficients $b_I(\boldsymbol{x},h)$ can be determined by solving the following matrix equation:

$$\begin{bmatrix} m_0(\boldsymbol{x},h) & m_1(\boldsymbol{x},h) & \cdots & m_k(\boldsymbol{x},h) \\ m_1(\boldsymbol{x},h) & m_2(\boldsymbol{x},h) & \cdots & m_{1+k}(\boldsymbol{x},h) \\ \vdots & \vdots & \ddots & \vdots \\ m_k(\boldsymbol{x},h) & m_{k+1}(\boldsymbol{x},h) & \cdots & m_{k+k}(\boldsymbol{x},h) \end{bmatrix} \begin{Bmatrix} b_0(\boldsymbol{x},h) \\ b_1(\boldsymbol{x},h) \\ \vdots \\ b_k(\boldsymbol{x},h) \end{Bmatrix} = \begin{Bmatrix} 1 \\ 0 \\ \vdots \\ 0 \end{Bmatrix}. \tag{32}$$

After determining the coefficients $b_I(\boldsymbol{x},h)$, the smoothing function expressed in Eq. (30) can be numerically calculated, which assures the discretized consistency to kth order. Therefore this particle consistency restoring process actually gives a new approach to construct some kind of numerical smoothing function for meshfree particle methods, and thus to provide a new way to solve the meshfree particle problem. This approach mathematically is very useful. The famous reproducing kernel particle method (RKPM) [8,9] is somewhat similar to this approach. In the RKPM, the reproducing kernel function $\bar{W}$ was developed by multiplying the function expressed in Eq. (30) with another window function $W_w(\boldsymbol{x}-\boldsymbol{x}_j,h)$ that is usually a traditional SPH smoothing function such as the cubic spline

$$\bar{W}(\boldsymbol{x}-\boldsymbol{x}_j,h)=W(\boldsymbol{x}-\boldsymbol{x}_j,h)W_w(\boldsymbol{x}-\boldsymbol{x}_j,h). \tag{33}$$

The $k+1$ coefficients $b_I(\boldsymbol{x},h)$ can be determined by solving the same Eq. (32) except that

$$m_k(\boldsymbol{x},h)=\sum_{j}^{N}\left(\frac{\boldsymbol{x}-\boldsymbol{x}_j}{h}\right)^k W_w(\boldsymbol{x}-\boldsymbol{x}_j,h)\Delta\boldsymbol{x}_j.$$

Comparing with the traditional smoothing function, which is only dependent on the particle distance, the resultant smoothing function is pointwise, and therefore depends on both the distance and position of the interacting particles. The cost-effectiveness for this approach in constructing pointwise smoothing function needs to be considered since it will require additional CPU time to solve the pointwise equation (32). Moreover since all particles are moving, the particle connectivity is changing as well. Another problem is that solving Eq. (32) implies the computation of the inverse of the coefficient matrix. It is clear that a non-zero value is required for the determinant of the coefficient matrix. To obtain non-zero determinant, the particle distribution must satisfy some kind of condition rather than the random distribution in the original SPH method.

As far as the interpolation is concerned, the restoring of particle consistency is a big improvement and will greatly enhance the simulation accuracy. However, it should be noted that restoring the consistency in discrete form leads to some special questions. Firstly, the resultant smoothing function is negative in some parts of the region; secondly, the resultant smoothing function may not be monotonically decreasing with the increase of the particle (node) distance; thirdly the function may not be symmetric. These violate the previously discussed properties of a traditional smoothing function and may result in some serious consequence. For example, negative smoothing function may yield unphysical value such as negative density, and again breakdown the entire computation.

3. Constructing the smoothing function

3.1. Constructing the smoothing function

As discussed earlier, the approach of restoring particle inconsistency actually gives a new way to construct numerical smoothing function. However, some questions may occur for the resultant pointwise smoothing function especially when simulating hydrodynamic problems. In our work, rather than using the discrete form of constructing conditions, we employ the continuous equations (22) and (23) to construct smoothing function, which is only dependent on the inter-particle distance, and can have analytical expression rather than numerical value based on the distribution of the neighbor particles. The constructed analytical smoothing function has special advantages especially for problems with randomly distributed particles and with statistical features where the determinant approach of constructing smoothing function through restoring particle consistency is difficult to apply.

If the smoothing function is assumed to be a polynomial dependent only on the relative distance of the concerned particles, it can be assumed to take the following form with an influencing width of κh,

$$W(\boldsymbol{x}-\boldsymbol{x}',h)=W(S)=a_0+a_1S+a_2S^2+\cdots+a_nS^n \tag{34}$$

where $S=|\boldsymbol{x}-\boldsymbol{x}'|/h$. So the smoothing function is an even function since it depends on the relative distance rather than the positions of the particles.

For Eq. (34), if $W^{(i)}(\boldsymbol{x}-\boldsymbol{x}',h)$ exists,

$$W^{(i)}(0)=\begin{cases} i!a_i, & \dfrac{\boldsymbol{x}-\boldsymbol{x}'}{h}\to 0_+,\\ (-1)^i i!a_i, & \dfrac{\boldsymbol{x}-\boldsymbol{x}'}{h}\to 0_-. \end{cases} \tag{35}$$

So $W^{(i+1)}(\boldsymbol{x}-\boldsymbol{x}',h)$ exists only if the following expressions are satisfied:

$$a_{1\to i}=0,\quad i=2k+1,\quad k=0,1,2\ldots,$$
$$a_{1\to i-1}=0,\quad i=2(k+1),\quad k=0,1,2\ldots. \tag{36}$$

In Eqs. (22)–(23), the first and second derivative of the smoothing function are involved. Therefore, for the second derivative of the smoothing function to exist, the term related to a_1 should vanish in Eq. (34)

$$W(\boldsymbol{x}-\boldsymbol{x}',h)=W(S)=a_0+a_2S^2+\cdots+a_nS^n. \tag{37}$$

Substituting W into the constructing conditions (22), (23), the parameters $a_0,a_2,\ldots,a_n$ can be calculated from the coupled linear equations, and then the smoothing function can be analytically determined. It can be seen that the resultant expression for the smoothing function can be used for general purpose, and does not need to resort to time consuming matrix inversion for each simulation case at each step.

3.2. Some special aspects

3.2.1. Non-negative smoothing function

As mentioned above the conditions expressed in Eqs. (22) and (23) provide a general approach to interpolate and to construct the smoothing functions. Similar to the particle consistency restoring approach, the smoothing function derived from the continuous kernel form, however, will not necessarily be positive especially when high order accuracy approximation is required. As far as the interpolation schemes are concerned, negative smoothing function can produce approximations with required accuracy. For these cases, the approximation may be called a somewhat smoothed point method rather than smoothing particle hydrodynamics.

However, the distinct advantage of the smoothed particle hydrodynamics over ordinary interpolation method lies in the Lagrangian nature, which moves the particles in response to the internal interactions and external forces. As far as the terminology hydrodynamics is concerned, the fluid is divided into and represented by a finite number of particles. The terminology particle is more suitable than terminology point since besides the volume, particles possess physical variables such as mass, density and so on. Under such hydrodynamic circumstances, negative smoothing function may result in unphysical solutions such as negative density (mass) and negative energy. For this purpose, the smoothing functions in the emerged literatures are generally non-negative. In sum, for the purpose of hydrodynamic simulations, the constructed smoothing functions for smoothed particle hydrodynamics should be non-negative. While according to Eq. (22), for even order ($k=2,4,6\ldots$) accuracy to be obtained, the smoothing function has to be negative in parts of the region. It seems one cannot have everything at the same time.

3.2.2. Center peak value

The center peak value of the smoothing function is very important since it determines how much the particle itself will contribute to the approximation. Since the smoothing function for smoothed particle hydrodynamics needs to be non-negative for hydrodynamic simulations, it is impossible to satisfy all the constructing conditions expressed in Eq. (22). It is observed that for a non-negative smoothing function, the constructing conditions of $\int W(\boldsymbol{x}-\boldsymbol{x}',h)\,\mathrm{d}\boldsymbol{x}'=1$, $\int(\boldsymbol{x}-\boldsymbol{x}')W(\boldsymbol{x}-\boldsymbol{x}',h)\,\mathrm{d}\boldsymbol{x}'=0$ and Eq. (23) can be satisfied, but $\int(\boldsymbol{x}-\boldsymbol{x}')^2W(\boldsymbol{x}-\boldsymbol{x}',h)\,\mathrm{d}\boldsymbol{x}'$ will not be satisfied if W is not always zero. So no matter if the later constructing conditions are satisfied or not, the highest order of accuracy for the function approximation is second order. Under such circumstances, the integration $\int(\boldsymbol{x}-\boldsymbol{x}')^2W(\boldsymbol{x}-\boldsymbol{x}',h)\,\mathrm{d}\boldsymbol{x}'$ can be used a mark to measure the accuracy of the function approximation. The lower the integration is, the more accurate the function approximation is. The center peak value of the smoothing function is closely related to $\int(\boldsymbol{x}-\boldsymbol{x}')^2W(\boldsymbol{x}-\boldsymbol{x}',h)\,\mathrm{d}\boldsymbol{x}$. Larger center peak value of the smoothing function means smaller value of the integration. Therefore as far as the SPH kernel approximation process is concerned, larger center peak value of the smoothing function means better accuracy. In constructing the smoothing function, the center peak value is a factor that needs to be considered, and can be designated in the constructing process.

3.2.3. Piecewise smoothing function

In some circumstances, the piecewise smoothing function is preferred since the shape of the piecewise smoothing function is easier to be controlled by changing the number of the pieces and the locations of the separation point. For example, consider a smoothing function with two pieces,

$$W(S)=\begin{cases} W_1(S), & 0\leqslant S<S_1,\\ W_2(S), & S_1\leqslant S<S_2,\\ 0, & S_2\leqslant S,\end{cases} \tag{38}$$

the function itself and the derivatives at the separation points should be continuous, so

$$W_1(S_1)=W_2(S_1),\quad W_1'(S_1)=W_2'(S_1),\quad W_1''(S_1)=W_2''(S_1). \tag{39}$$

Considering the requirements at the separation points as well as the compact supportness, one possible form of the smoothing function is

$$W(S)=\begin{cases} b_1(S_1-S)^n+b_2(S_2-S)^n, & 0\leqslant S<S_1,\\ b_2(S_2-S)^n, & S_1\leqslant S<S_2,\\ 0, & S_2\leqslant S.\end{cases} \tag{40}$$

For more pieces, similar expressions can be used to construct the smoothing functions.

3.3. Some examples of constructed smoothing functions

3.3.1. Dome-shaped quadratic smoothing function

If the smoothing function is a quadratic expression of S, and the scale factor $\kappa=1$, in one dimensional space, the resultant smoothing kernel is $W(S,h)=3/4h(1-S^2)$ (Fig. 2), which was used for the grid free finite interpolation method (FIM) by Hicks and Liebrock [5].

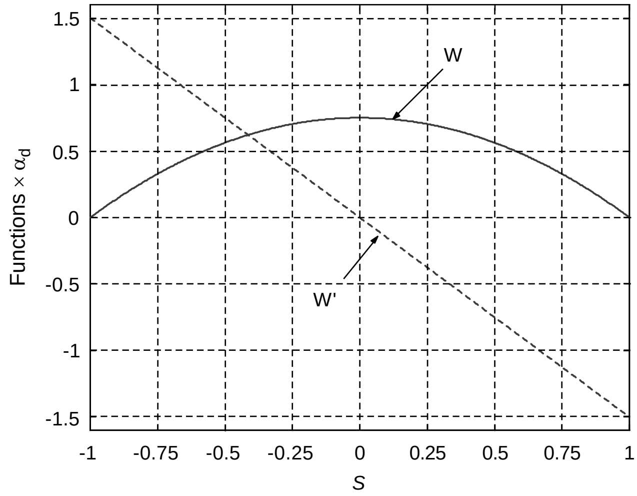

Fig. 2. Dome-shaped quadratic kernel and its first derivative.

3.3.2. Piecewise cubic smoothing function

If the smoothing function is a piecewise cubic function with the separation point at $S=1$ and $\kappa=2$, the smoothing function can also take the form expressed in Eq. (40). By using the first expression in Eq. (22) and considering the existence of the second derivative of the smoothing function, the resultant parameters $b_1=\frac{1}{6}$, $b_2=-\frac{2}{3}$. The constructed piecewise cubic smoothing function is exactly the most commonly used cubic spline smoothing function in SPH literatures [12,15] (Fig. 3),

$$W(S,h)=\alpha_{\rm d}\times\begin{cases}\dfrac{2}{3}-S^2+\dfrac{1}{2}S^3, & 0\leqslant S<1,\\ \dfrac{1}{6}(2-S)^2, & 1\leqslant S<2,\\ 0, & S\geqslant 2.\end{cases} \tag{41}$$

In one, two or three dimensional space, $\alpha_{\rm d}=1/h,\ 15/7\pi h^2,\ 3/2\pi h^3$ respectively.

3.3.3. Piecewise quintic smoothing function

If the smoothing function is a piecewise quintic function with the separation point at $S_1=1$ and $S_2=2$, the scale factor $\kappa=3$, the smoothing function can also take the similar form expressed in Eq. (40). By using the first expression in Eq. (22), considering the existence of the second derivative of the smoothing function, and defining the center peak value, the resultant parameters $b_1=1$, $b_2=-6$, and $b_3=15$. $\alpha_{\rm d}$ is $1/120h$, $7/478\pi h^2$ and $3/359\pi h^3$ in one, two and three dimensions, respectively. The constructed smoothing function (Fig. 4) is the one employed by Morris [17] in simulating low

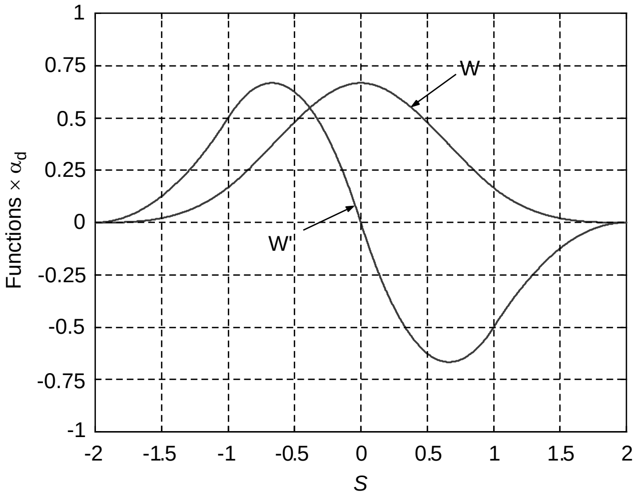

Fig. 3. Cubic spline kernel and its first derivative.

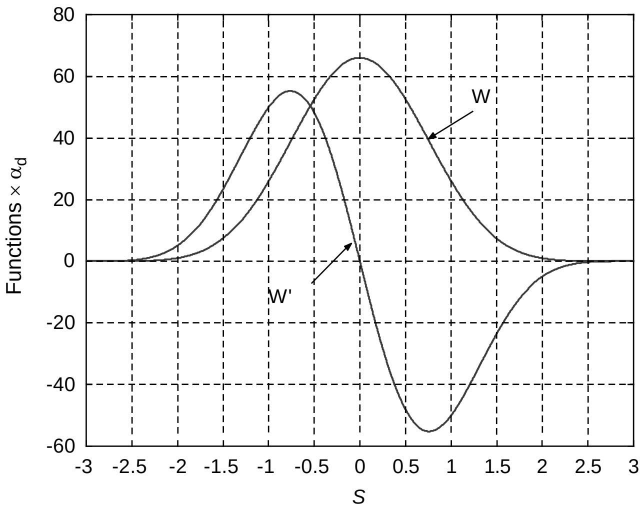

Fig. 4. Quintic kernel and its first derivative.

Reynolds number incompressible flow.

$$W(S,h) = \alpha_d \times \begin{cases} (3-S)^5 - 6(2-S)^5 + 15(1-S)^5, & 0 \leqslant S < 1, \\ (3-S)^5 - 6(2-S)^5, & 1 \leqslant S < 2, \\ (3-S)^5, & 2 \leqslant S < 3, \\ 0, & S > 3. \end{cases} \tag{42}$$

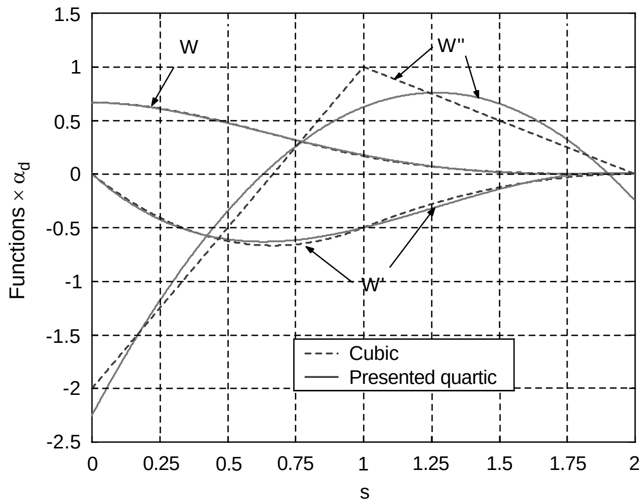

Fig. 5. The new quartic smoothing function and its first two derivatives.

3.3.4. A new quartic smoothing function

By using the same idea, a new quartic smoothing function is constructed as follows

$$W(S,h) = \begin{cases} \alpha_d \left(\dfrac{2}{3} - \dfrac{9}{8}S^2 + \dfrac{19}{24}S^3 - \dfrac{5}{32}S^4 \right), & 0 \leqslant S \leqslant 2, \\ 0, & S > 2, \end{cases} \tag{43}$$

where α_d is $1/h$, $15/7\pi h^2$ and $315/208\pi h^3$ in one, two and three dimensions, respectively. The quartic smoothing function and its first two derivatives are shown in Fig. 5. The presented quartic function satisfies the normalization condition, the function itself and first derivative have compact support. The presented quartic function is very close to the most commonly used cubic spline (Eq. (41)) with the same center peak value of $\frac{2}{3}$, and monotonically decreases with the increase of the distance. The new quartic function has several advantages over the cubic function. Considering the integration of $\int (\boldsymbol{x} - \boldsymbol{x}')^2 W(\boldsymbol{x} - \boldsymbol{x}', h)\, \mathrm{d}\boldsymbol{x}'$, the presented quartic function yields smaller values than that from the cubic smoothing function, and therefore as far as the kernel approximation is concerned, the quartic function produces better results. Since the stability properties of SPH depend strongly on the second derivative of the smoothing function [21,16], a smoother smoothing function generally results in more stable SPH formulations. The presented quartic function has smoother second derivative than the piecewise linear second derivative of the cubic function, and therefore the stability properties should be superior to those of the cubic function.

4. Numerical examples

The effectiveness of the approach in constructing smoothing functions has been shown in the above different smoothing functions. The efficiency and accuracy of the constructed smoothing functions have also been verified in various literatures. Presented here are two numerical tests for the newly constructed quartic function.

4.1. Shock tube problem

The shock tube problem is a good numerical benchmark and was comprehensively investigated by many SPH researchers when studying SPH [4,14], in which the cubic spline function is employed as the smoothing function. The shock-tube is a tube filled with gas, which is separated by a membrane into two parts of different pressures and densities. The gas in each part is initially in an equilibrium state. When taking away the membrane suddenly, a shock wave is produced and moves into the lower density gas, a rarefaction wave travels into the higher density gas, a contact discontinuity forms near the center and travels into the low-density region behind the shock.

In this work, the newly constructed quartic function is used as the smoothing function to simulate this shock tube problem. The initial conditions are similar to what Hernquist [4] used, which was introduced by Monaghan [14] from [20].

$$x \leqslant 0, \quad \rho = 1, \quad \boldsymbol{v} = 0, \quad u = 2.5, \quad p = 1, \quad \Delta x = 0.001875,$$

$$x > 0, \quad \rho = 0.25, \quad \boldsymbol{v} = 0, \quad u = 1.795, \quad p = 0.1795, \quad \Delta x = 0.0075,$$

where ρ, p, u and $\boldsymbol{v}$ are the density, pressure, internal energy, and velocity of the gas respectively. Δx is the inter-particle distances.

There are 400 particles used in the simulation. All particles have the same mass of $m_i = 0.001875$. 320 particles are evenly distributed in the high-density region $[-0.6, 0.0]$, and 80 particles in the low-density region [0.0, 0.6]. The purpose of this initial particle distribution is to obtain required discontinuous density profile in the computing area. The equation of state for the ideal gas $p = (\gamma - 1)\rho u$ is accepted in the simulation with $\gamma = 1.4$. The time step is 0.005 and the simulation ran for 30 time steps. In resolving the shock, the Monaghan type artificial viscosity [12] is used, which also solves to prevent unphysical penetration. Figs. 6–9 show the density, pressure, velocity and internal energy profiles. It can be seen the obtained results from the new approach agree well with the exact solution in the region $[-0.4, 0.4]$. The shock is observed from $x = 0.2$ to 0.25; and is resolved within several smoothing lengths. The rarefaction wave is located between $x = -0.2$ and 0. The contact discontinuity is around $x = 0.1$. The boundary is not specially treated since for the instant at $t = 0.15$ s, the boundary effect has not propagated to the shock area, and therefore the shock physics is not affected by the boundary effect.

4.2. One dimensional high explosive detonation

The HE detonation process involves in a violent chemical reaction which converts the original high energy explosive charge into gas at very high temperature and pressure, occurring with extreme rapidity and releasing a great deal of heat. One important benchmark in HE detonation simulation is a one dimensional TNT slab detonation [10,19], in which a 0.1 m long TNT slab detonates at one end of the TNT slab. The newly constructed quartic smoothing function is used to simulate this one dimensional TNT detonation problem. In the simulation, the JWL equation of state for the detonation produced high explosive gas is used. The detonation velocity D of TNT is 6930 m/s.

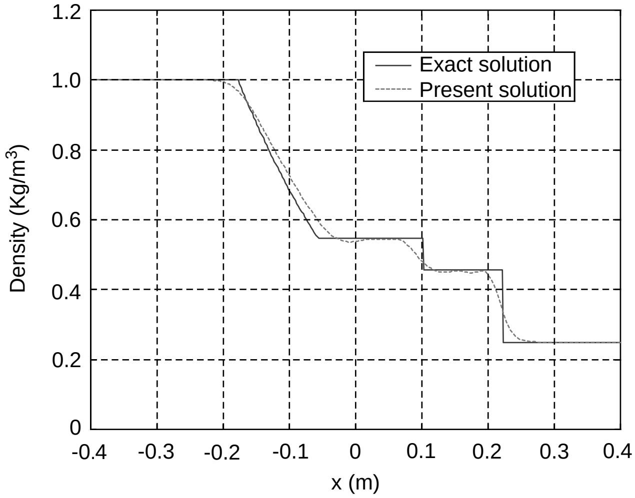

Fig. 6. Density profiles for the shock tube.

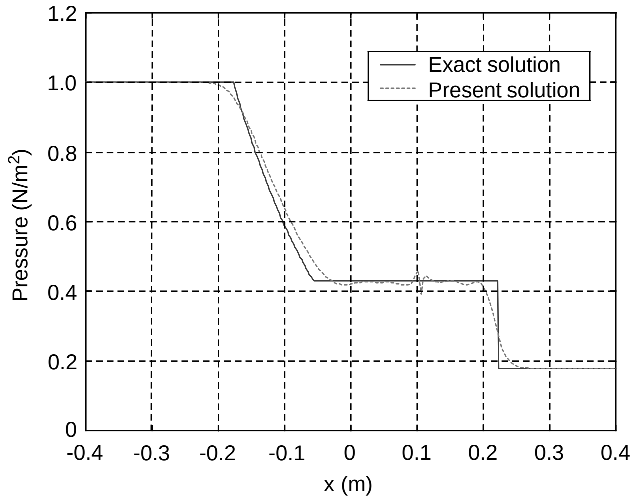

Fig. 7. Pressure profiles for the shock tube.

If the solid wall boundary condition is used to forbid material transport from everywhere, a symmetric setup can be employed to deploy the particles, and thus makes the detonation of the 0.1 m long slab from one end to the other end equivalent to the detonation of a 0.2 m long slab from the middle point to both ends. Before detonation, particles are evenly distributed along the slab. The initial smoothing length is one and a half times the particle separation. After detonation, a plane detonation wave is produced. According to the detonation velocity, it takes around 14.4 μs to complete the detonation to the end of the slab. Fig. 10 shows the pressure profile along the slab

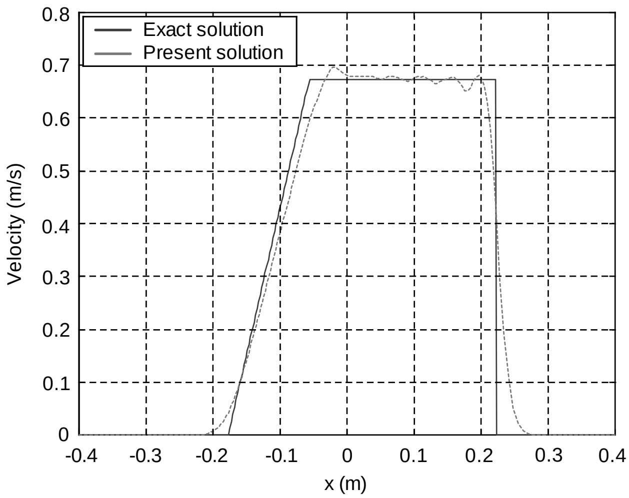

Fig. 8. Velocity profiles for the shock tube.

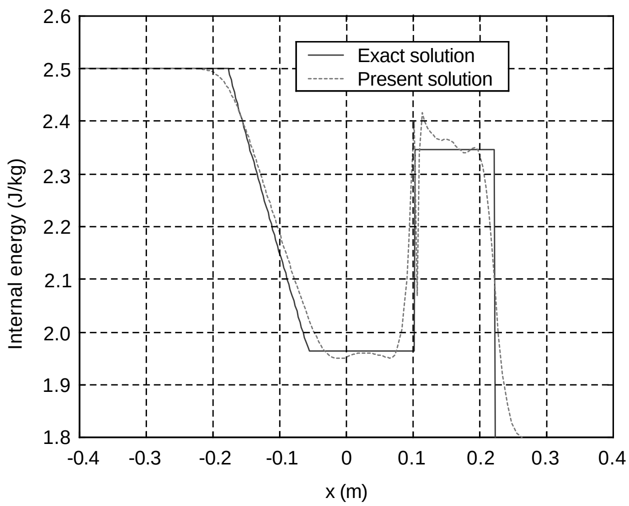

Fig. 9. Internal energy profiles for the shock tube.

at 1 μs interval from 1 to 14 μs by using 4000 particles. The dashed line in Fig. 10 represents the experimentally determined C–J detonation pressure, which is, according to the Chapman and Jouguet's hypothesis, the pressure at the tangential point of the Hugoniot curve and the Rayleigh line, and represents the pressure at the equilibrium plane at the trailing edge of the very thin chemical reaction zone. For this one dimensional TNT slab detonation problem, the experimental C–J pressure is 2.1×10^{10} N/m^2. It can be seen from Fig. 10 that, with the process of the detonation, the detonation pressure converges to the C–J pressure. If the free boundary applies, the explosive

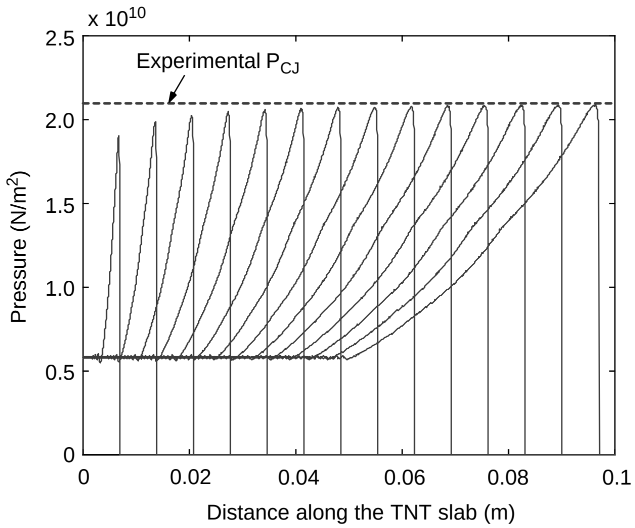

Fig. 10. Pressure profiles along the TNT slab during the detonation process.

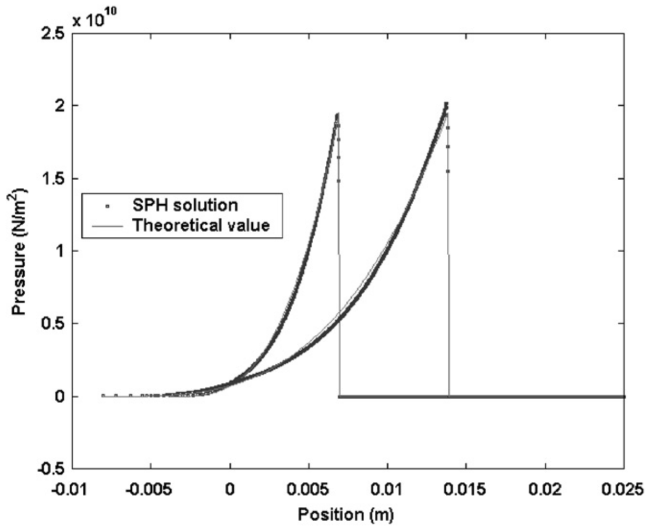

Fig. 11. Pressure transients at 1 and 2 μs.

gas behind the C–J plane disperses outwards with the forward propagating detonation wave. Figs. 11–13 show the comparisons of pressure, density and velocity profiles between theoretical values [22] and the presented SPH results at 1 and 2 μs. The close agreement between the SPH results and the theoretical solutions verifies the validity of the newly constructed smoothing function.

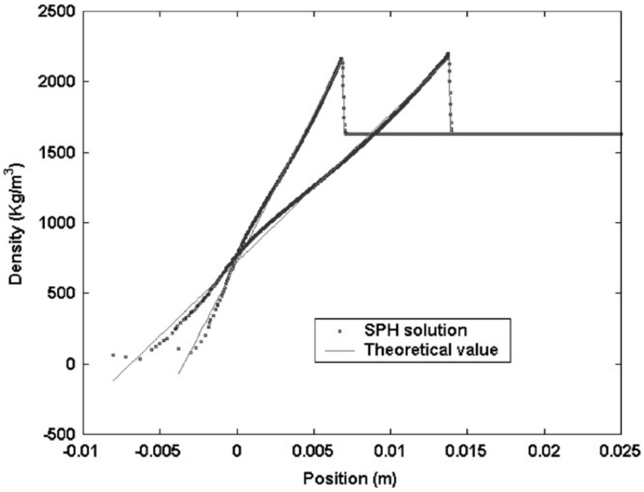

Fig. 12. Density transients at 1 and 2 μs.

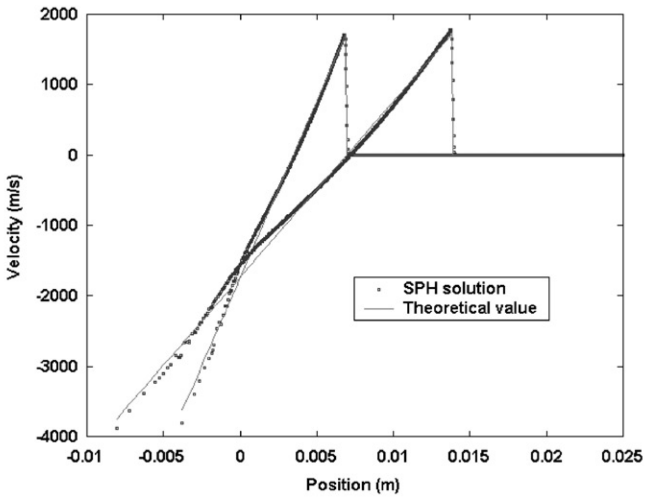

Fig. 13. Velocity transients at 1 and 2 μs.

5. Concluding remarks

The smoothing function is significant in smoothed particle hydrodynamics since it determines the pattern of the interpolation and the effective influencing area of a certain particle. In this paper, based on the Taylor series expansion to the SPH formulations for function and derivative approximation, an approach of constructing smoothing functions is generalized. The constructing conditions are systematically derived, which make clear that the former requirements on the smoothing function are actually representation of SPH approximations for the function and its derivatives. The constructing conditions interpret the consistency conditions and the compact supportness. The particle consistency can be restored through constructing a pointwise numerical smoothing function.

The constructing conditions in continuous kernel form provide a general approach to devise analytical smoothing function. The constructed analytical smoothing function is not location dependent, and may be used in other meshless particle method. Though there is no requirement on the sign of the smoothing function mathematically, it should be noted that negative values should be avoided to prevent from obtaining unphysical results when the method is applied to simulate hydrodynamic problems. The center peak value of the smoothing function also should be considered since the value is related to the accuracy to the SPH kernel approximation. Piecewisely constructing the smoothing function is also feasible if proper considerations on the separation points can be appropriately considered. With this more general approach, some examples of smoothing functions are constructed including some existing ones. A quartic smoothing function with some advantages is also constructed and applied to simulate the one dimensional shock tube problem and a one dimensional high explosive detonation problem with a good agreement with the solution from the other sources.

References

[1] E. Asphaug, Kevin Olson, Impacts into asteroids and planets: parallel tree code simulations using smooth particle hydrodynamics, WWW address: http://sdcd.gsfc.nasa.gov/ESS/annual.reports/ess98/asphaug.html

[2] P.W. Cleary, Modelling confined multi-material heat and mass flows using SPH, Appl. Math. Modell. 22 (1998) 981–993.

[3] R.A. Gingold, J.J. Monaghan, Smoothed particle hydrodynamics: theory and application to non-spherical stars, Mon. Not. R. Astron. Soc. 181 (1977) 375–389.

[4] L. Hernquist, N. Katz, TreeSPH—A unification of SPH with the hierarchical tree method, Astrophys. J. Ser. (Suppl.) 70 (1989) 419–446.

[5] D.L. Hicks, L.M. Liebrock, Lanczo's generalized derivative: insights and applications, Appl. Math. Comput. 112 (2000) 63–73.

[6] G.R. Johnson, R.A. Stryk, S.R. Beissel, SPH for high velocity impact computations, Comput. Methods Appl. Mech. Eng. 139 (1996) 347–373.

[7] L.D. Liberskty, A.G. Petsheck, et al., High strain Lagrangian hydrodynamics-a three-dimensional SPH code for dynamic material response, J. Comput. Phys. 109 (1993) 67–75.

[8] W.K. Liu, S. Jun, S. Li, J. Adee, T. Belytschko, Reproducing kernel particle methods for structural dynamics, Int. J. Numer. Methods Eng. 38 (1995) 1655–1679.

[9] W.K. Liu, S. Jun, Y.F. Zhang, Reproducing kernel particle methods, J. Numer. Methods Eng. 20 (1995) 1081–1106.

[10] M.B. Liu, G.R. Liu, Z. Zong, K.Y. Lam, Computer simulation of the high explosive explosion using smoothed particle hydrodynamics methodology, Comput. Fluids 32 (3) (2003) 305–322.

[11] L.B. Lucy, Numerical approach to testing the fission hypothesis, Astron. J. 82 (1977) 1013–1024.

[12] J.J. Monaghan, Smoothed particle hydrodynamics, Annu. Rev. Astron. Astrophys. 30 (1992) 543–574.

[13] J.J. Monaghan, Simulating free surface flows with SPH, J. Comput. Phys. 110 (1994) 399–406.

[14] J.J. Monaghan, R.A. Gingold, Shock simulation by the particle method of SPH, J. Comput. Phys. 52 (1983) 374–381.

[15] J.J. Monaghan, J.C. Lattanzio, A refined particle method for astrophysical problems, Astron. Astrophys. 149 (1985) 135–143.

[16] J.P. Morris, Analysis of smoothed particle hydrodynamics with applications, Ph.D. Thesis, Monash University, 1996.

[17] J.P. Morris, P.J. Fox, Y. Zhu, Modeling low Reynolds number incompressible flows using SPH, J. Comput. Phys. 136 (1997) 214–226.

[18] S.J. Plimpton, S. Attaway, B. Hendrickson, J. Swegle, C. Vaughan, D. Gardner, Parallel transient dynamics simulations: algorithms for contact detection and smoothed particle hydrodynamics, J. Parallel. Distrib. Comput. 50 (1998) 104–122.
[19] Y.S. Shin, J.E. Chisum, Modeling and simulation of underwater shock problems using a coupled Lagrangian–Eulerian analysis approach, Shock Vib. 4 (1997) 1–10.
[20] G.A. Sod, A survey of several finite difference methods for systems of hyperbolic conservation laws, J. Comput. Phys. 27 (1978) 1–31.
[21] J.W. Swegle, D.L. Hicks, S.W. Attaway, Smoothed particle hydrodynamics stability analysis, J. Comput. Phys. 116 (1) (1995) 123–134.
[22] S.Z. Zhang, et al., Detonation and its applications, Press of National Defense Industry, Beijing, 1976.
[23] M.B. Liu, G.R. Liu, K.Y. Lam, Investigations into water mitigations using a meshless particle method, Shock Waves 12 (3) (2002) 181–195.